Forces acting on a small particle in an acoustical field in a viscous fluid

Mikkel Settnes and Henrik Bruus
Department of Micro- and Nanotechnology, Technical University of Denmark, DTU Nanotech Building 345 B, DK-2800 Kongens Lyngby, Denmark

(Received 27 October 2011; revised manuscript received 6 January 2012; published 30 January 2012)

We calculate the acoustic radiation force from an ultrasound wave on a compressible, spherical particle suspended in a viscous fluid. Using Prandtl-Schlichting boundary-layer theory, we include the kinematic viscosity of the solvent and derive an analytical expression for the resulting radiation force, which is valid for any particle radius and boundary-layer thickness provided that both of these length scales are much smaller than the wavelength of the ultrasound wave (millimeters in water at megahertz frequencies). The acoustophoretic response of suspended microparticles is predicted and analyzed using parameter values typically employed in microchannel acoustophoresis.

DOI: 10.1103/PhysRevE.85.016327 PACS number(s): 47.15.Rq, 43.25.Qp, 43.20.Fn

I. INTRODUCTION

Particles suspended in acoustic fields are subject to time-averaged forces from scattering of the acoustic waves. Theoretical studies of these forces, known as acoustic radiation forces, date back to King in 1934, who considered incompressible particles suspended freely in an inviscid fluid [1]. In 1955 Yosioka and Kawasima extended the analysis to include the compressibility of the suspended particles [2]. These results were summarized and generalized by a simple and physically intuitive method by Gorkov in 1962 [3], but limited to inviscid fluids and particles smaller than the acoustic wavelength λ.

With recent developments in microfabrication technologies allowing for integration of ultrasound resonators in lab-on-a-chip systems, the acoustic radiation force has received renewed attention as a label- and contact-free way to manipulate particles. Several biotechnological applications of particle trapping and separation have been reported where ultrasound resonances in microchannels were used to create acoustic fields giving rise to acoustic radiation forces on suspended particles. Examples are on-chip acoustophoretic cell separation devices [4–6], cell trapping [7–9], plasmapheresis [10], forensic analysis [11], food analysis [12], cell sorting using surface acoustic waves [13], cell synchronization [14], cell differentiation [15], and cell compressibility studies [16]. At the same time, substantial advancements in understanding the fundamental physics of biochip acoustophoresis have been achieved through full-chip imaging of acoustic resonances [17], particle handling by surface acoustic waves [18–22], multiresonance chips [23], advanced frequency control [24,25], on-chip integration with magnetic separators [26], acoustics-assisted microgrippers [27], acoustic programming [28], band-pass filters [29], *in situ* force calibration [30], and automated micro-PIV systems [31]. See also the recent reviews on acoustofluidics [32,33].

Traditionally, the acoustic radiation force has been modeled using the inviscid theory of the acoustic radiation force. This approach is approximately correct for particles significantly larger than the thickness δ of the acoustic boundary layer, in which viscosity does play a dominant role. For a fluid with kinematic viscosity (or momentum diffusivity) ν and with an acoustic field of angular frequency ω, the boundary layer thickness (or viscous penetration depth) is the momentum diffusion length δ given by Refs. [34,35]

$$\delta = \sqrt{\frac{2\nu}{\omega}} \approx 0.6\,\mu\mathrm{m}, \tag{1}$$

where the value is for 1-MHz ultrasound in water at room temperature. It is therefore expected that particles or cells with a radius larger than 3 μm can be described fairly accurately by the inviscid theory. However, as the technological development pushes for higher accuracy, more refined applications, and the handling of smaller particles, it becomes relevant to calculate the effects on acoustophoresis from viscosity of the solvent.

We are not the first to analyze how the acoustic radiation force depends on δ. However, the earlier works by Doinikov [36] and by Danilov and Mironov [37] focus mainly on developing general theoretical schemes for particles of radius a smaller than the wavelength λ and only provide analytical expressions in the special limits $\delta \ll a \ll \lambda$ and $a \ll \delta \ll \lambda$. However, given the length scale above, the range of applicability of the published expressions for viscous corrections is *a priori* severely limited. The aim of this paper is to provide an analytical expression for the viscous corrections to the acoustic radiation force on small suspended particles $\delta, a \ll \lambda$, and to analyze its implications for experimentally relevant parameters central for current studies in the field of microchannel acoustophoresis of compressible particles in liquids.

We begin by establishing the governing equations for acoustophoresis in the framework of second-order perturbation theory of the Navier-Stokes equation in the acoustic field. Then, following the inviscid analysis by Gorkov [3], we express the radiation force on a particle in terms of the far-field solution of inviscid acoustic wave scattering theory, extend this solution to the near-field region close to the particle, and match it with the solution to the incompressible viscous flow problem in the acoustic boundary layer of the particle. From this we obtain the analytical expression for the acoustic radiation force in the viscous case. Finally, we analyze the predictions of the theory for experimentally relevant parameter values.

II. PERTURBATION EXPANSION OF THE GOVERNING EQUATIONS

The formulation of the governing equations for acoustics in perturbation theory is well known, and the reader is referred to the textbooks by Landau and Lifshitz [35], Lighthill [38], and Pierce [39]. Briefly and to establish notation [40], for a given fluid in the absence of external forces and for isothermal conditions, the theory is based on a combination of the thermodynamic equation of state expressing pressure p in terms of density ρ, the kinematic continuity equation for ρ, and the dynamic Navier-Stokes equation for the velocity field $\boldsymbol{v}$,

$$p = p(\rho), \tag{2a}$$

$$\partial_t \rho = -\boldsymbol{\nabla}\cdot(\rho\boldsymbol{v}), \tag{2b}$$

$$\rho\partial_t \boldsymbol{v} = -\boldsymbol{\nabla} p - \rho(\boldsymbol{v}\cdot\boldsymbol{\nabla})\boldsymbol{v} + \eta\nabla^2\boldsymbol{v} + \beta\eta\,\boldsymbol{\nabla}(\boldsymbol{\nabla}\cdot\boldsymbol{v}), \tag{2c}$$

where η is the dynamic viscosity of the fluid and β the viscosity ratio typically of the order of unity. Thermal effects are neglected because the thermal diffusion length in liquids is much smaller than the momentum diffusion length (or viscous penetration depth) δ, see Ref. [36].

We consider a quiescent liquid, which before the presence of any acoustic wave has constant density ρ_0 and pressure p_0. Let an acoustic wave constitute tiny perturbations to first and second order (subscript 1 and 2, respectively) in density ρ, pressure p, and velocity $\boldsymbol{v}$,

$$\rho = \rho_0 + \rho_1 + \rho_2, \tag{3a}$$

$$p = p_0 + c_0^2\rho_1 + p_2, \tag{3b}$$

$$\boldsymbol{v} = \boldsymbol{v}_1 + \boldsymbol{v}_2. \tag{3c}$$

Here we have introduced the speed of sound c_0 of the fluid, the square of which is given by the (isentropic) derivative $c_0^2 = (\partial p/\partial\rho)_s$, ensuring the useful identity

$$p_1 = c_0^2\rho_1, \tag{4}$$

and an explicit expression for the compressibility κ_0,

$$\kappa_0 = -\frac{1}{V}\frac{\partial V}{\partial p} = \frac{1}{\rho_0}\frac{\partial\rho}{\partial p} = \frac{1}{\rho_0 c_0^2}. \tag{5}$$

It is a fundamental, unproven, assumption in perturbation theory that the expansion terms in Eq. (3) get successively smaller and that the sums including all orders converge [35,38,39]. However, for most of the acoustophoretic applications mentioned in Sec. I, the acoustic energy density even at resonance is $E_{\mathrm{ac}} < 10^2\,\mathrm{J/m^3}$, corresponding to $|\rho_1|/\rho_0 = |v_1|/c_0 < 10^{-3}$. Moreover, the observed time-averaged acoustic streaming velocities $|\langle v_2\rangle|$ are typically of the order $100\,\mu\mathrm{m/s}$, which is a factor 10^{-4} smaller than $|v_1|$. Given the smallness of these ratios, the perturbation expansion is expected to be valid, but the reader is referred to Ref. [32] for a review over cases where the perturbation expansion is questionable.

The first-order perturbation (or linearization) of the continuity and Navier-Stokes equation is

$$\partial_t\rho_1 = -\rho_0\boldsymbol{\nabla}\cdot\boldsymbol{v}_1, \tag{6a}$$

$$\rho_0\partial_t\boldsymbol{v}_1 = -c_0^2\boldsymbol{\nabla}\rho_1 + \eta\nabla^2\boldsymbol{v}_1 + \beta\eta\,\boldsymbol{\nabla}(\boldsymbol{\nabla}\cdot\boldsymbol{v}_1). \tag{6b}$$

The first-order acoustic wave equation for ρ_1 is obtained by taking the time derivative ∂_t of Eq. (6a) followed by insertion of Eq. (6b) in the resulting expression,

$$\partial_t^2\rho_1 = c_0^2\left[1 + \frac{(1+\beta)\eta}{\rho_0 c_0^2}\partial_t\right]\nabla^2\rho_1. \tag{7}$$

For acoustics fields in the bulk, that is, at distances much greater than δ from rigid boundaries, the viscous dissipation is negligible because of the minute damping coefficient $\eta\omega/(\rho_0 c_0^2) \ll 1$, where ω is a characteristic angular frequency of the system. However, the bulk field is disturbed by the no-slip boundary condition forcing the velocity of the fluid at any rigid wall to equal the velocity of that wall. This disturbance is decaying exponentially away from the wall with δ as the decay length [see, e.g., Eq. (36)] and large velocity gradients may occur in Eq. (6b), such that $\eta v_1/\delta^2 \gtrsim \rho_0\partial_t v_1$, and viscosity cannot be neglected. Since the exponential decay drops below 1% at a distance of 5δ, we take this as the thickness of the acoustic boundary layer, however the precise value of the prefactor is not important, see Sec. IV B.

The acoustic radiation force is a time-average effect that does not resolve the oscillatory behavior of the acoustic fields, so in this work we do not need the full second-order perturbation of the governing equations, but only their time average. We assume that after the vanishing of transients, any first-order field $f(\boldsymbol{r},t)$ has a harmonic time dependence,

$$f(\boldsymbol{r},t) = f(\boldsymbol{r})\,\mathrm{e}^{-\mathrm{i}\omega t}, \tag{8}$$

and define the time average $\langle X\rangle$ over a full oscillation period τ of a quantity $X(t)$ as

$$\langle X\rangle \equiv \frac{1}{\tau}\int_0^\tau dt\; X(t). \tag{9}$$

From this we obtain the time-averaged, second-order perturbation of Eqs. (2b) and (2c) in the form

$$\rho_0\boldsymbol{\nabla}\cdot\langle\boldsymbol{v}_2\rangle = -\boldsymbol{\nabla}\cdot\langle\rho_1\boldsymbol{v}_1\rangle, \tag{10a}$$

$$-\boldsymbol{\nabla}\langle p_2\rangle + \eta\nabla^2\langle\boldsymbol{v}_2\rangle + \beta\eta\boldsymbol{\nabla}(\boldsymbol{\nabla}\cdot\langle\boldsymbol{v}_2\rangle) = \langle\rho_1\partial_t\boldsymbol{v}_1\rangle + \rho_0\langle(\boldsymbol{v}_1\cdot\boldsymbol{\nabla})\boldsymbol{v}_1\rangle. \tag{10b}$$

We note that the physical, real-valued time average $\langle f\,g\rangle$ of two harmonically varying fields f and g with the complex representation Eq. (8), is given by the real-part rule

$$\langle f\,g\rangle = \tfrac{1}{2}\mathrm{Re}[f(\boldsymbol{r})\,g^*(\boldsymbol{r})], \tag{11}$$

where the asterisk denotes complex conjugation.

Clearly the time-averaged, second-order fields will in general be nonzero, as the nonvanishing time-averaged products of first-order terms act as source terms on the right-hand side in the governing equations.

In the inviscid bulk, the first-order flow $\boldsymbol{v}_1$ is a potential flow, see Eq. (6b) with $\eta = 0$, which when used in Eq. (10b) and combined with Eq. (5) leads to

$$\langle p_2\rangle = \tfrac{1}{2}\kappa_0\langle p_1^2\rangle - \tfrac{1}{2}\rho_0\langle v_1^2\rangle. \tag{12}$$

III. THE ACOUSTIC RADIATION FORCE

We are analyzing the acoustic radiation force on a compressible, spherical, micrometer-sized particle of radius

a suspended in a viscous fluid in an ultrasound field of wavelength λ (=1 mm in water at room temperature for $\omega/2\pi = 1.5$ MHz), thus $a \ll \lambda$. In terms of acoustic waves, the microparticle thus acts as a weak point scatterer, which we will treat by first-order scattering theory. In response to an incoming wave, described by the oscillatory velocity field $\boldsymbol{v}_{\rm in}$, an outgoing wave $\boldsymbol{v}_{\rm sc}$ propagates away from the particle, and the first-order acoustic velocity field $\boldsymbol{v}_1$ is given by the sum

$$\boldsymbol{v}_1 = \boldsymbol{v}_{\rm in} + \boldsymbol{v}_{\rm sc}. \tag{13}$$

Once the first-order scattered field $\boldsymbol{v}_{\rm sc}$ have been determined for a given incoming first-order field $\boldsymbol{v}_{\rm in}$, the acoustic radiation force $\boldsymbol{F}^{\rm rad}$ on the particle can be calculated as the time-averaged second-order forces acting on a fixed surface $\partial\Omega$ in the inviscid bulk, encompassing the particle [3]. Momentum conservation and zero bulk forces ensures that any fixed surface can be chosen. For inviscid fluids, $\boldsymbol{F}^{\rm rad}$ is the sum of the time-averaged second-order pressure $\langle p_2\rangle$ and momentum flux tensor $\rho_0\langle \boldsymbol{v}_1\boldsymbol{v}_1\rangle$,

$$\begin{aligned}\boldsymbol{F}^{\rm rad} &= -\int_{\partial\Omega} da\, \{\langle p_2\rangle \boldsymbol{n} + \rho_0\langle(\boldsymbol{n}\cdot\boldsymbol{v}_1)\boldsymbol{v}_1\rangle\} \\ &= -\int_{\partial\Omega} da \left\{\left[\frac{\kappa_0}{2}\langle p_1^2\rangle - \frac{\rho_0}{2}\langle v_1^2\rangle\right]\boldsymbol{n} + \rho_0\langle(\boldsymbol{n}\cdot\boldsymbol{v}_1)\boldsymbol{v}_1\rangle\right\}. \end{aligned} \tag{14}$$

To ease the determination of p_1 and $\boldsymbol{v}_1$, we use that in the inviscid bulk, they can be expressed in terms of a velocity potential ϕ_1 as $\boldsymbol{v}_1 = \nabla\phi_1$ and $p_1 = -\rho_0\partial_t\phi_1$. For a harmonic time dependence, Eq. (6b) implies

$$\phi_1 = -\mathrm{i}\,\frac{c_0^2}{\rho_0\omega}\,\rho_1, \tag{15}$$

and, as sketched in Fig. 1(a), we henceforth write

$$\phi_1 = \phi_{\rm in} + \phi_{\rm sc}, \tag{16a}$$
$$\boldsymbol{v}_1 = \nabla\phi_1 = \nabla\phi_{\rm in} + \nabla\phi_{\rm sc}, \tag{16b}$$
$$p_1 = \mathrm{i}\,\rho_0\omega\,\phi_1 = \mathrm{i}\,\rho_0\omega\,\phi_{\rm in} + \mathrm{i}\,\rho_0\omega\,\phi_{\rm sc}. \tag{16c}$$

By virtue of Eqs. (7) and (15), ϕ_1 (as well as $\phi_{\rm in}$ and $\phi_{\rm sc}$) obeys the inviscid wave equation $\partial_t^2\phi = c_0^2\nabla^2\phi$ in the bulk. As we can use any surface $\partial\Omega$ to calculate the radiation force $\boldsymbol{F}^{\rm rad}$, the simplest choice is a surface in the far-field region $r \gg \lambda$, where the spherical particle of radius a is placed at the center of the coordinate system, and where $\boldsymbol{r}$ is a position vector. According to standard scattering theory [35,41,42], the scattered field $\phi_{\rm sc}$ from a point scatterer can be represented by a time-retarded multipole expansion. In the far-field region, the monopole component and dipole components dominate, $\phi_{\rm sc} \approx \phi_{\rm mp} + \phi_{\rm dp}$, and in general, these two components have the specific forms $\phi_{\rm mp}(\boldsymbol{r},t) = b(t - r/c_0)/r$ and $\phi_{\rm dp}(\boldsymbol{r},t) = \nabla\cdot[\boldsymbol{B}(t - r/c_0)/r]$, where b is a scalar function and $\boldsymbol{B}$ a vector function of the retarded argument $t - r/c_0$. In first-order scattering theory, $\phi_{\rm sc}$ must be proportional to the first-order fields determined by $\phi_{\rm in}$. On physical grounds, the only relevant scalar field is the density, $b \sim \rho_{\rm in}$, or equivalently the pressure $p_{\rm in}$, while the only relevant vector field is the velocity $\boldsymbol{B} \sim \boldsymbol{v}_{\rm in}$. Here both $\rho_{\rm in}$ and $\boldsymbol{v}_{\rm in}$ are evaluated at the particle position with time-retarded arguments, and in the far-field region $\phi_{\rm sc}$ must therefore have the form

$$\begin{aligned}\phi_{\rm sc}(\boldsymbol{r},t) = &-f_1\frac{a^3}{3\rho_0}\frac{\partial_t\rho_{\rm in}(t - r/c_0)}{r} \\ &- f_2\frac{a^3}{2}\nabla\cdot\left[\frac{\boldsymbol{v}_{\rm in}(t - r/c_0)}{r}\right], \quad r \gg \lambda, \end{aligned} \tag{17}$$

where the particle radius a, the unperturbed density ρ_0, and the time derivative ∂_t are introduced to ensure the correct physical dimension of $\phi_{\rm sc}$, namely m^2/s. The factors $1/3$ and $1/2$ are inserted for later convenience.

Before reaching the main goal of the calculation, namely the determination of the dimensionless scattering coefficients f_1 and f_2, the radiation force $\boldsymbol{F}^{\rm rad}$ is expressed in terms of the incoming acoustic wave $\phi_{\rm in}$ at the particle position and the coefficients f_1 and f_2. When inserting the velocity potentials Eqs. (16a) and (17) into Eq. (14) for $\boldsymbol{F}^{\rm rad}$, we obtain a sum

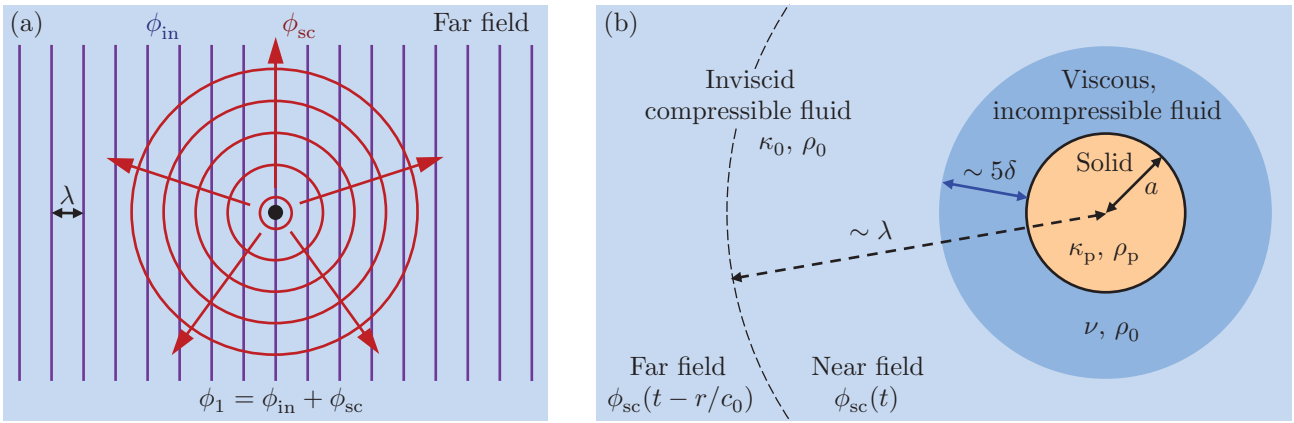

FIG. 1. (Color online) (a) Sketch of the far-field region $r \gg \lambda$ of an incoming acoustic wave $\phi_{\rm in}$ (vertical lines) of wavelength λ scattering off a small particle (black dot) with radius $a \ll \lambda$, leading to the outgoing scattered wave $\phi_{\rm sc}$ (circles and arrows). The resulting first-order wave is $\phi_1 = \phi_{\rm in} + \phi_{\rm sc}$. (b) Sketch of a compressible spherical particle of radius a, compressibility $\kappa_{\rm p}$, and density $\rho_{\rm p}$, surrounded by the incompressible, viscous acoustic boundary layer of width $\sim 5\delta$ (dark shade) with density ρ_0 and kinematic viscosity ν. Outside is the compressible inviscid bulk (light shade) of compressibility κ_0 and density ρ_0. The bulk liquid is divided into the near-field region for $r \ll \lambda$, with the instantaneous scattered field $\phi_{\rm sc}(t)$, and the far-field region with time-retarded scattered field $\phi_{\rm sc}(t - r/c_0)$.

of terms each proportional to the square of $\phi_1 = \phi_{\rm in} + \phi_{\rm sc}$. This results in three types of contributions, (i) squares of $\phi_{\rm in}$ containing no information about the scattering and therefore yielding zero, (ii) squares of $\phi_{\rm sc}$ proportional to the square of the particle volume a^6 and therefore negligible compared to (iii) the mixed products $\phi_{\rm in}\phi_{\rm sc}$ proportional to particle volume a^3, which are the dominant contributions to $\boldsymbol{F}^{\rm rad}$. Keeping only these mixed terms representing interference between the incoming and the scattered wave, we have in Appendix A derived the following expression for $\boldsymbol{F}^{\rm rad}$ in terms of the incoming velocity field $\boldsymbol{v}_{\rm in}$ and the scattered potential $\phi_{\rm sc}$,

$$\boldsymbol{F}^{\rm rad} = -\int_\Omega d\boldsymbol{r}\; \rho_0 \left\langle \boldsymbol{v}_{\rm in}\left(\nabla^2 - \frac{1}{c_0^2}\partial_t^2\right)\phi_{\rm sc}\right\rangle. \tag{18}$$

As shown in Appendix A the appearance of the d'Alembert wave operator $\nabla^2 - (1/c_0^2)\partial_t^2$ acting on $\phi_{\rm sc}$ leads to significant simplification. In particular, the integrand turns out to be proportional to the Dirac δ function $\delta(\boldsymbol{r})$ being singular at the position of the particle center. Combining this with some vector theorems and a partial integration (for details see Appendix A), we arrive at the resulting expression for $\boldsymbol{F}^{\rm rad}$,

$$\boldsymbol{F}^{\rm rad} = -\pi a^3\left[\frac{2\kappa_0}{3}{\rm Re}[f_1^* p_{\rm in}^* \nabla p_{\rm in}] - \rho_0 {\rm Re}[f_2^* \boldsymbol{v}_{\rm in}^* \cdot \nabla \boldsymbol{v}_{\rm in}]\right], \quad \text{with } p_{\rm in} \text{ and } \boldsymbol{v}_{\rm in} \text{ evaluated at } \boldsymbol{r} = \boldsymbol{0}. \tag{19}$$

For standing waves $\phi_{\rm in}$, the spatial part $f(\boldsymbol{r})$ of the incoming fields $f(\boldsymbol{r})e^{i\omega t}$ is real, so the nabla operator in Eq. (19) does not lead to any phase changes. Consequently, the radiation force acting on a small particle ($a \ll \lambda$) placed in a standing wave is a gradient force of the following form:

$$\boldsymbol{F}^{\rm rad} = -\nabla U^{\rm rad} \quad \text{for a standing wave } \phi_{\rm in}, \tag{20a}$$

$$U^{\rm rad} = \frac{4\pi}{3}a^3\left[{\rm Re}[f_1]\frac{\kappa_0}{2}\langle p_{\rm in}^2\rangle - {\rm Re}[f_2]\frac{3\rho_0}{4}\langle v_{\rm in}^2\rangle\right]. \tag{20b}$$

The radiation potential $U^{\rm rad}$ is proportional to the volume of the particle, and it contains a positive contribution from the acoustic pressure fluctuations and a negative contribution originating from the Bernoulli effect of the acoustic flow speed squared.

For traveling waves, the spatial part $f(\boldsymbol{r})$ of the incoming fields $f(\boldsymbol{r})e^{i\omega t}$ contains a phase changing factor, for example, the plane-wave factor $e^{i\boldsymbol{k}\cdot\boldsymbol{r}}$ or the spherical-wave factor e^{ikr}, which changes the overall structure of the resulting radiation force. Assuming for simplicity an incoming plane wave with wave number $\boldsymbol{k}$ parallel to $\boldsymbol{v}_{\rm in}$, we have $\nabla p_{\rm in} = i\boldsymbol{k}p_{\rm in}$ and $\nabla \boldsymbol{v} = i\boldsymbol{k}\boldsymbol{v}$, and Eq. (A3d) leads to a resulting radiation force of the form

$$\boldsymbol{F}^{\rm rad} = \frac{4\pi}{3}a^3\left[{\rm Im}[f_1]\frac{\kappa_0}{2}\langle p_{\rm in}^2\rangle + {\rm Im}[f_2]\frac{3\rho_0}{4}\langle v_{\rm in}^2\rangle\right]\boldsymbol{k} \quad \text{for a traveling wave } \phi_{\rm in}. \tag{21}$$

Note that this is not a gradient force.

IV. THE SCATTERING COEFFICIENTS

The scattering coefficients f_1 and f_2 of Eq. (17) are found by matching the pressure p_1 and velocity $\boldsymbol{v}_1$ of the fluid with the boundary conditions at the particle moving with the instantaneous velocity $\boldsymbol{v}_{\rm p}$. In the following we use a spherical coordinate system with unit vectors $(\boldsymbol{e}_r, \boldsymbol{e}_\theta, \boldsymbol{e}_\phi)$ located at the instantaneous center of the particle. Due to the azimuthal symmetry of the problem, all fields depend only on r and θ, and the velocities has no azimuthal component, $\boldsymbol{v} = v_r\boldsymbol{e}_r + v_\theta\boldsymbol{e}_\theta$. The polar axis $\boldsymbol{e}_z$ points along the instantaneous direction of the incoming velocity $\boldsymbol{v}_{\rm in}$, such that $\boldsymbol{v}_{\rm in} = v_{\rm in}\boldsymbol{e}_z$. By the azimuthal symmetry of the problem, the particle must also move in that direction, $\boldsymbol{v}_{\rm p} = v_{\rm p}\boldsymbol{e}_z$,

$$\boldsymbol{v}_{\rm in} = v_{\rm in}\boldsymbol{e}_z = \cos\theta\; v_{\rm in}\boldsymbol{e}_r - \sin\theta\; v_{\rm in}\boldsymbol{e}_\theta, \tag{22a}$$

$$\boldsymbol{v}_{\rm p} = v_{\rm p}\boldsymbol{e}_z = \cos\theta\; v_{\rm p}\boldsymbol{e}_r - \sin\theta\; v_{\rm p}\boldsymbol{e}_\theta. \tag{22b}$$

As sketched in Fig. 1(b), the response of the fluid is different in three regions of space [35]. Just outside the sphere, in the so-called acoustic boundary layer given by $a < r \lesssim a + 5\delta$, viscosity is important due to the increased shear gradients in the velocity fields, as discussed after Eq. (7). Moreover, the fluid appears incompressible since the time it takes an acoustic wave to propagate across the boundary layer around the particle is much less than the oscillation period, $(a + 5\delta)/c_0 \ll 1/\omega$ or $a + 5\delta \ll \lambda$. The first-order pressure and velocity fields in the viscous and incompressible acoustic boundary layer are denoted $p_{\rm ab}$ and $\boldsymbol{v}_{\rm ab}$, respectively. In the next region, the so-called near-field region with $a + 5\delta \lesssim r \ll \lambda$, the fluid is inviscid and compressible, but $\phi_{\rm sc}$ depends on the instantaneous argument t and not the time-retarded argument $t - r/c_0$. The scattering potential Eq. (17) with its monopole and dipole term becomes

$$\phi_{\rm sc}(r,\theta) = \phi_{\rm mp}(r) + \phi_{\rm dp}(r,\theta), \quad a + 5\delta \lesssim r \ll \lambda, \tag{23a}$$

$$\phi_{\rm mp}(r) = -f_1\frac{a^3}{3\rho_0}\partial_t\rho_{\rm in}\frac{1}{r}, \tag{23b}$$

$$\phi_{\rm dp}(r,\theta) = +f_2\frac{a^3}{2}v_{\rm in}\frac{\cos\theta}{r^2}. \tag{23c}$$

Finally, outermost in the far-field region $r \gg \lambda$, the fluid is inviscid and compressible with a time-retarded $\phi_{\rm sc}$.

In first-order scattering theory the monopole and dipole parts of the problem do not mix: f_1 is the coefficient in the monopole scattering potential $\phi_{\rm mp}$ from a stationary sphere in the incoming density wave $\rho_{\rm in}$, while f_2 is the coefficient in the dipole scattering potential $\phi_{\rm dp}$ from an incompressible sphere moving with velocity $\boldsymbol{v}_{\rm p}$ in the incoming velocity wave $\boldsymbol{v}_{\rm in}$.

A. The monopole scattering coefficient f_1

The presence of a stationary, compressible particle causes a mass rate $\partial_t m$ of fluid to be ejected, that would otherwise have entered the particle volume. To first order, the ejection is determined by the mass flux $\rho_0\boldsymbol{v}_{\rm sc}$ carried by the scattered wave through a surface $\partial\Omega$ encompassing the particle in the near-field region. For a spherical surface with surface vector $\boldsymbol{n} = \boldsymbol{e}_r$ we obtain

$$\partial_t m = \int_{\partial\Omega} da\; \boldsymbol{e}_r \cdot (\rho_0\boldsymbol{v}_{\rm sc}) = f_1\,\frac{4\pi}{3}a^3\,\partial_t\rho_{\rm in}. \tag{24}$$

The factor $1/3$ was introduced in Eq. (17) to make the particle volume $V_p = (4\pi/3)a^3$ appear here. The rate of ejected mass can also be written in terms of the rate of change

of the incoming density $\rho_0 + \rho_{\rm in}$ multiplied by the particle volume V_p as $\partial_t m = \partial_t[(\rho_0 + \rho_{\rm in})V_p]$. Expressing this through the compressibility $\kappa = -(1/V)(\partial V/\partial p)$ of the fluid κ_0, and the particle $\kappa_{\rm p}$, we obtain

$$\partial_t m = \left[1 - \frac{\kappa_{\rm p}}{\kappa_0}\right] V_p \, \partial_t \rho_{\rm in}. \tag{25}$$

Now, f_1 is obtained by equating Eqs. (24) and (25),

$$f_1(\tilde{\kappa}) = 1 - \tilde{\kappa}, \quad \text{with} \quad \tilde{\kappa} = \frac{\kappa_{\rm p}}{\kappa_0}. \tag{26}$$

This result is identical to that of Gorkov [3]. We note that f_1 is real valued and depends only on the compressibility ratio $\tilde{\kappa}$ between the particle and the fluid; the viscosity of the fluid does not influence the compressibility and mass ejection. For identical compressibilities, $\tilde{\kappa} = 1$, the monopole scattering vanishes, $f_1(1) = 0$.

B. The dipole scattering coefficient f_2

As f_2 is related to the translational motion of the particle, it depends on the viscosity of the fluid, and we must therefore explicitly calculate the first-order velocity $\boldsymbol{v}_{\rm ab}(r,\theta)$ in the viscous, acoustic boundary layer $a < r \lesssim a + 5\delta$. This velocity must match the dipole part $\boldsymbol{v}_{\rm in} + \boldsymbol{\nabla}\phi_{\rm dp}$ of the fluid velocity in the near-field region $r \ll \lambda$, see Eqs. (22a) and (23c). Because of the separation of length scales the matching can be made at a distance $r \approx r^*$ fulfilling $a + 5\delta \ll r^* \ll \lambda$, and this so-called asymptotic matching [35,43] is written

$$\boldsymbol{e}_r \cdot \boldsymbol{v}_{\rm ab}(r \approx r^*,\theta) = \left[1 - f_2 \frac{a^3}{r^3}\right] \cos\theta \; v_{\rm in}, \tag{27a}$$

$$\boldsymbol{e}_\theta \cdot \boldsymbol{v}_{\rm ab}(r \approx r^*,\theta) = \left[1 + \frac{1}{2} f_2 \frac{a^3}{r^3}\right] (-\sin\theta) \; v_{\rm in}. \tag{27b}$$

At the surface of the sphere, $r = a$, the no-slip boundary condition requires $\boldsymbol{v}_{\rm ab}$ to equal $\boldsymbol{v}_{\rm p}$ of Eq. (22b),

$$\boldsymbol{e}_r \cdot \boldsymbol{v}_{\rm ab}(a,\theta) = \cos\theta \; v_{\rm p}, \tag{28a}$$

$$\boldsymbol{e}_\theta \cdot \boldsymbol{v}_{\rm ab}(a,\theta) = (-\sin\theta) \; v_{\rm p}. \tag{28b}$$

The velocity $v_{\rm p}$ of the sphere is given by Newton's second law with $\partial_t v_{\rm p} = -{\rm i}\omega v_{\rm p}$ and with the viscous stress from the fluid acting on the surface of the sphere,

$$\begin{aligned} -{\rm i}\frac{4}{3}\pi \, a^3 \rho_{\rm p} \omega \, v_{\rm p} &= \int_{\partial V_{\rm p}} da \, \boldsymbol{n} \cdot \boldsymbol{\sigma}_{\rm ab} \cdot \boldsymbol{e}_z \\ &= 2\pi \, a^2 \int_{-1}^{1} d(\cos\theta) \big[\big(- p_{\rm ab} + \tilde{\sigma}^{\rm ab}_{rr} \big) \cos\theta - \tilde{\sigma}^{\rm ab}_{\theta r} \sin\theta \big]. \end{aligned} \tag{29}$$

The viscous stress components are $\tilde{\sigma}^{\rm ab}_{rr} = 2\eta\partial_r v^{\rm ab}_r$ and $\tilde{\sigma}^{\rm ab}_{\theta r} = \eta[(1/r)\partial_\theta v^{\rm ab}_r + \partial_r v^{\rm ab}_\theta - (1/r)v^{\rm ab}_\theta]$.

The determination of the pressure $p_{\rm ab}$ and velocity field $\boldsymbol{v}_{\rm ab}$ is eased by the incompressibility of the fluid in the acoustic boundary layer $\boldsymbol{\nabla} \cdot \boldsymbol{v}_{\rm ab} = 0$. Taking the divergence of the first-order Navier-Stokes equation (6b), leads to the Laplace equation of the pressure $\nabla^2 p_{\rm ab} = 0$. Since we are seeking the dipole solution, and since $p_{\rm ab}$ must match asymptotically with the dipole part ${\rm i}\rho_0\omega(\phi_{\rm in} + \phi_{\rm dp})$ of Eqs. (16c) and (23), we can directly write the pressure inside the boundary layer as

$$p_{\rm ab}(r,\theta) = {\rm i}\rho_0\omega \left[r + \frac{1}{2}\frac{a^3}{r^2} f_2 \right] \cos\theta \; v_{\rm in}, \tag{30a}$$

$$p_{\rm ab}(a,\theta) = {\rm i}\rho_0\omega a \left[1 + \frac{1}{2} f_2 \right] \cos\theta \; v_{\rm in}. \tag{30b}$$

For the velocity field, incompressibility combined with the azimuthal symmetry of the problem, implies that $\boldsymbol{v}_{\rm ab}$ can be written in terms of a stream function $\Psi(r,\theta)$ as

$$\boldsymbol{v}_{\rm ab}(r,\theta) = \boldsymbol{\nabla} \times [\Psi(r,\theta) \, \boldsymbol{e}_\phi], \tag{31}$$

where Ψ depends only on r and θ but is multiplied with the azimuthal unit vector $\boldsymbol{e}_\phi$. As shown in Appendix B, by taking the rotation of the first-order Navier-Stokes equation (6b), the stream function can be written as a sum $\Psi = \Psi_1 + \Psi_2$. The first term Ψ_1 satisfies the equation

$$\nabla^2 \Psi_1 - \frac{\Psi_1}{r^2 \sin^2\theta} = 0, \tag{32}$$

for which the dipole part of the solution is of the (long range) Legendre form $\Psi_1(r,\theta) = A_1 r \cos\theta + A_2 \cos\theta / r^2$. The second term Ψ_2 satisfies the equation

$$\nabla^2 \Psi_2 - \frac{\Psi_2}{r^2 \sin^2\theta} = -q^2 \Psi_2, \quad \text{with} \quad q = \frac{1+{\rm i}}{\delta}, \tag{33}$$

for which the dipole part of the solution is the (decaying) Hankel form $\Psi_2(r,\theta) = B h^1_1(qr) \, a v_{\rm in} \sin\theta$, where $h^1_1(s) = -{\rm e}^{{\rm i}s}({\rm i}s + 1)/s^2$ is the spherical Hankel function of the first kind (outgoing wave) of order 1. Note that all information about the viscosity resides within the parameter q, and since $h^1_1(qr) \propto {\rm e}^{{\rm i}qr} \propto {\rm e}^{-r/\delta}$ decays exponentially on the length scale δ, the viscous, acoustic boundary layer can be ascribed the aforementioned thickness of $\sim 5\delta$. An important, dimensionless parameter for the analysis is therefore the ratio $\tilde{\delta}$ of the viscous penetration length δ and the particle radius a,

$$\tilde{\delta} = \frac{\delta}{a}. \tag{34}$$

To find the explicit form of Ψ, we first determine the constants A_1 and A_2 by the asymptotic matching conditions (27), $\boldsymbol{v}_{\rm ab}(r \approx r^*,\theta) = \boldsymbol{\nabla} \times [\Psi_1 \boldsymbol{e}_\phi]$, and obtain

$$\Psi_1(r,\theta) = \left[\frac{1}{2} r - \frac{f_2}{2} \frac{a^3}{r^2} \right] \sin\theta \; v_{\rm in}. \tag{35}$$

Combining this with $\boldsymbol{v}_{\rm ab} = \boldsymbol{\nabla} \times [(\Psi_1 + \Psi_2)\boldsymbol{e}_\phi]$ yields

$$\boldsymbol{v}_{\rm ab} \cdot \boldsymbol{e}_r = \left[1 - f_2 \frac{a^3}{r^3} + 2qaB \left(\frac{h^1_1(s)}{s} \right)_{qr} \right] \cos\theta \; v_{\rm in}, \tag{36a}$$

$$\boldsymbol{v}_{\rm ab} \cdot \boldsymbol{e}_\theta = \left[1 + \frac{f_2}{2} \frac{a^3}{r^3} + qaB \left\{ \frac{\partial_s (s h^1_1(s))}{s} \right\}_{qr} \right] (-\sin\theta) v_{\rm in}, \tag{36b}$$

leaving the constant B to be determined. Inserting $\boldsymbol{v}_{\rm ab}$ of Eq. (36) into the no-slip condition at the surface of the sphere [Eq. (28)] and inserting the pressure $p_{\rm ab}$ of Eq. (30b) together with $\boldsymbol{v}_{\rm ab}$ into Newton's second law for the sphere

[Eq. (29)], we arrive at three equations for the three unknowns f_2, v_p, and B,

$$v_p = \left[1 - f_2 + 2Bh_1^1(qa)\right] v_{in}, \tag{37a}$$

$$v_p = \left[1 + \tfrac{1}{2}f_2 + B\partial_s\left(sh_1^1(s)\right)_{qa}\right] v_{in}, \tag{37b}$$

$$\tilde{\rho} v_p = \left[1 + \tfrac{1}{2}f_2 + 2Bh_1^1(qa)\right] v_{in}. \tag{37c}$$

By subtracting Eq. (37a) from Eq. (37b), B is found in terms of f_2 and the factor $\partial_s(sh_1^1(s)) - 2h_1^1(s) = sh_0^1(s) - 3h_1^1(s)$, where $h_0^1(s) = -(\mathrm{i}/s)\mathrm{e}^{\mathrm{i}s}$ is the spherical Hankel function of the first kind of order 0. It is helpful to introduce the dimensionless, $\tilde{\delta}$-dependent variable γ as

$$\gamma(\tilde{\delta}) = \frac{3h_1^1(qa)}{qah_0^1(qa)} = -\frac{3}{2}[1 + \mathrm{i}(1 + \tilde{\delta})]\tilde{\delta}. \tag{38}$$

By straightforward algebra, f_2 is found from Eq. (37),

$$f_2(\tilde{\rho},\tilde{\delta}) = \frac{2[1 - \gamma(\tilde{\delta})](\tilde{\rho} - 1)}{2\tilde{\rho} + 1 - 3\gamma(\tilde{\delta})}, \quad \text{with} \quad \tilde{\rho} = \frac{\rho_p}{\rho_0}. \tag{39}$$

The viscosity-dependent dipole scattering coefficient f_2 is in general a complex-valued number, and its real and imaginary values are abbreviated as

$$f_2^{\mathrm{r}}(\tilde{\rho},\tilde{\delta}) = \mathrm{Re}[f_2(\tilde{\rho},\tilde{\delta})], \tag{40a}$$

$$f_2^{\mathrm{i}}(\tilde{\rho},\tilde{\delta}) = \mathrm{Im}[f_2(\tilde{\rho},\tilde{\delta})]. \tag{40b}$$

In the absence of viscosity $\tilde{\delta} = 0$ we recover the real-valued result by Gorkov [3],

$$f_2(\tilde{\rho},0) = \frac{2(\tilde{\rho} - 1)}{2\tilde{\rho} + 1}. \tag{41}$$

Physically, this result for an inviscid fluid can also be derived directly from Eq. (37): The acoustic boundary layer vanishes, $B = 0$, and the condition (37b) on the tangential velocity component is dropped, so we are left with the normal-component condition (37a), $v_p = (1 - f_2)v_{in}$, and Newton's second law (37c), $\tilde{\rho} v_p = (1 + \frac{1}{2}f_2)v_{in}$, from which Eq. (41) follows.

The nonzero imaginary part f_2^{i} of f_2 for $\tilde{\delta} > 0$ implies that for a traveling wave ϕ_{in} the product terms $\phi_{in}\phi_{sc}$ of order a^3 remain finite. This is in contrast to the inviscid case, where these terms vanish and the radiation force is reduced by a factor of $(ka)^3 = (2\pi a/\lambda)^3$ since only the quadratic terms ϕ_{sc}^2 proportional to a^6 remain finite [2,3]. In agreement with Doinikov [36], our analysis thus predicts the possibility of realizing a radiation force for traveling waves, which is a factor of $(ka)^{-3} = (\lambda/2\pi a)^3$ stronger than expected from the standard inviscid theory.

C. Properties of f_2

As the dipole scattering coefficient f_2, in contrast to the monopole coefficient f_1, depends on viscosity, we study some of its properties in more detail below and in Fig. 2. Importantly,

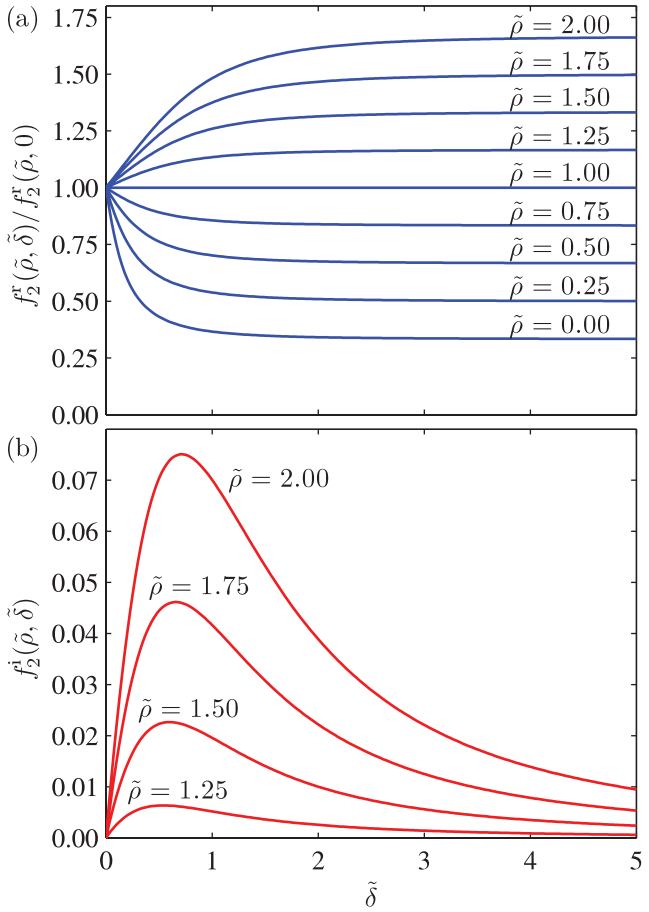

FIG. 2. (Color online) (a) The real part of the viscosity-dependent dipole scattering coefficient relative to its inviscid counterpart $f_2^{\mathrm{r}}(\tilde{\rho},\tilde{\delta})/f_2^{\mathrm{r}}(\tilde{\rho},0)$ plotted vs the nondimensionalized thickness $\tilde{\delta}$ of the viscous, acoustic boundary layer. (b) The imaginary part $f_2^{\mathrm{i}}(\tilde{\rho},\tilde{\delta})$ vs $\tilde{\delta}$ for $\tilde{\rho} = 1.25$, 1.50, 1.75, and 2.00. For the same parameters $0.17 < f_2^{\mathrm{r}}(\rho,\infty) < 0.67$.

f_2 is zero for neutral-buoyancy particles ($\tilde{\rho} = 1$) irrespective of the viscosity,

$$f_2(1,\tilde{\delta}) = 0, \tag{42}$$

and generally small for near-neutral-buoyancy particles.

For a large particle in a low-viscosity fluid $\tilde{\delta} \ll 1$, the correction to the Gorkov expression for f_2 is found by Taylor-expanding Eq. (39) to first order in $\tilde{\delta}$,

$$f_2(\tilde{\rho},\tilde{\delta} \ll 1) \approx \frac{2(\tilde{\rho} - 1)}{2\tilde{\rho} + 1}\left[1 + \frac{3(\tilde{\rho} - 1)}{2\tilde{\rho} + 1}(1 + \mathrm{i})\,\tilde{\delta}\right], \tag{43}$$

in agreement with Doinikov [36]. In earlier work by Weiser and Apfel [44] (building on Urick [45]) the numerator of the viscous correction was found to be $(9/2)\tilde{\delta}$ instead of $3(\tilde{\rho} - 1)\tilde{\delta}$. However, this discrepancy is due to an imprecise treatment of the viscous boundary layer in the earlier work.

For a small particle in a high-viscosity fluid $\tilde{\delta} \gg 1$, the viscosity dependence saturates, as the particle essentially becomes a point singularity at the center of the acoustic boundary, and f_2 becomes

$$f_2(\tilde{\rho},\tilde{\delta} \gg 1) \approx \tfrac{2}{3}(\tilde{\rho} - 1). \tag{44}$$

Doinikov presented the same expression except for the overall sign. This may be a misprint in his paper, as the consequence would otherwise be an unphysical reversal of the sign of the force as $\tilde{\delta}$ is increased from zero to infinity.

In Fig. 2(a) is shown plots of the real part $f_2^{\mathrm{r}}(\tilde{\rho},\tilde{\delta})$ of the viscosity-dependent dipole scattering coefficient relative to the inviscid coefficient $f_2^{\mathrm{r}}(\tilde{\rho},0)$ as a function of $\tilde{\delta}$ for different values of $\tilde{\rho}$ between 0 and 2. For these values of $\tilde{\rho}$ the values of $f_2^{\mathrm{r}}(\tilde{\rho},\tilde{\delta})/f_2^{\mathrm{r}}(\tilde{\rho},0)$ fall in the range from 0.3 to 1.7, and the saturation of f_2^{r} sets in for moderate values of $\tilde{\delta}$ between 1 and 2.

In Fig. 2(b) is shown the imaginary part $f_2^{\mathrm{i}}(\tilde{\rho},\tilde{\delta})$,

$$f_2^{\mathrm{i}}(\tilde{\rho},\tilde{\delta}) = \frac{6(1-\tilde{\rho})^2(1+\tilde{\delta})\tilde{\delta}}{(1+2\tilde{\rho})^2+9(1+2\tilde{\rho})\tilde{\delta}+\frac{81}{2}\left(\tilde{\delta}^2+\tilde{\delta}^3+\frac{1}{2}\tilde{\delta}^4\right)}, \tag{45}$$

with

$$f_2^{\mathrm{i}}(\tilde{\rho},\tilde{\delta}\ll 1) \approx \frac{6(1-\tilde{\rho})^2}{(1+2\tilde{\rho})^2}\,\tilde{\delta}, \tag{46a}$$

$$f_2^{\mathrm{i}}(\tilde{\rho},\tilde{\delta}\gg 1) \approx \frac{24}{81}(1-\tilde{\rho})^2\,\tilde{\delta}^{-2}. \tag{46b}$$

It exhibits a marked maximum for $\tilde{\delta}\approx 0.5$ with an amplitude roughly one order of magnitude smaller than the saturation value of $f_2^{\mathrm{r}}(\tilde{\rho},\infty)$ [Eq. (44)] for the corresponding densities $\tilde{\rho}$.

D. Resulting expressions for the radiation force

In summary, the main result of the paper are the following analytical expressions for the acoustic radiation force $\boldsymbol{F}^{\mathrm{rad}}$ on a spherical particle of radius a, density ρ_{p}, and compressibility κ_{p} suspended in a fluid of density ρ_0, compressibility κ_0, and viscosity η, and exposed to a first-order standing and traveling acoustic wave p_{in} and $\boldsymbol{v}_{\mathrm{in}}$ in the long wavelength limit $\lambda \gg a$.

For a standing acoustic wave we have obtained

$$\boldsymbol{F}^{\mathrm{rad}} = -\boldsymbol{\nabla} U^{\mathrm{rad}}, \tag{47a}$$

$$U^{\mathrm{rad}} = \frac{4\pi}{3}\,a^3\left[f_1\,\frac{1}{2}\kappa_0\left\langle p_{\mathrm{in}}^2\right\rangle - f_2^{\mathrm{r}}\,\frac{3}{4}\rho_0\left\langle v_{\mathrm{in}}^2\right\rangle\right], \tag{47b}$$

$$f_1(\tilde{\kappa}) = 1-\tilde{\kappa}, \quad \text{with} \quad \tilde{\kappa} = \frac{\kappa_{\mathrm{p}}}{\kappa_0}, \tag{47c}$$

$$f_2^{\mathrm{r}}(\tilde{\rho},\tilde{\delta}) = \mathrm{Re}\left[\frac{2[1-\gamma(\tilde{\delta})](\tilde{\rho}-1)}{2\tilde{\rho}+1-3\gamma(\tilde{\delta})}\right], \quad \text{with} \quad \tilde{\rho} = \frac{\rho_{\mathrm{p}}}{\rho_0}, \tag{47d}$$

$$\gamma(\tilde{\delta}) = -\frac{3}{2}\mathrm{Re}[1+\mathrm{i}(1+\tilde{\delta})]\tilde{\delta}, \quad \text{with} \quad \tilde{\delta} = \frac{\delta}{a}, \tag{47e}$$

and for a traveling planar wave with wave vector $\boldsymbol{k}$,

$$\boldsymbol{F}^{\mathrm{rad}} = f_2^{\mathrm{i}}(\tilde{\rho},\tilde{\delta})\,\pi a^3\rho_0\left\langle v_{\mathrm{in}}^2\right\rangle\boldsymbol{k}, \tag{48}$$

where $f_2^{\mathrm{i}}(\tilde{\rho},\tilde{\delta})$ is given by Eq. (45).

V. EXPERIMENTAL IMPLICATIONS

A. Typical materials

In practical applications, especially involving biological samples, the solvents are often aqueous salt solutions. Among these, sodium chloride (NaCl) solutions are arguably the ones best characterized acoustically, so we use this solvent as one of our model liquids in the following analysis. In Appendix C the current best values of the speed of sound c_{scs}, the density ρ_{scs}, and the viscosity η_{scs} of sodium chloride solutions (scs) are given as a function of temperature T (in °C) and mass fraction S of NaCl in the solution (salinity). To study the effects of change in viscosity we also include calculations with glycerol (gl) and with percoll (pc), a solution of polyvinylpyrrolidone-coated silica nanoparticles for which the speed of sound is nearly the same as for pure water [46], see Table I.

TABLE I. List of values of material parameters at 20 °C for typical liquids [water (wa), NaCl solution (scs), percoll (pc), glycerol (gl)] and solids [pyrex (PY), polystyrene (PS), polymethacrylate (PM), melamine resin (MR), a representative biological cell (Cell)] used in microchannel acoustophoresis.

Material	Density ρ (kg/m^3)	Compress. κ (1/TPa)	Longitud. speed of sound c (m/s)	Viscosity η (mPa s)
wa[a]	998.2	456	1482	1.002
scs[b]	1071	365	1599	1.170
pc[c]	1130	390	1507	100
gl[a]	1261	219	1904	1412
PY[a]	2230	27.8	5674	–
PS[c]	1050	172	2350	–
PM[c]	1190	148	2380	–
MR[c]	1510	67.5	3132	–
Cell[d]	1100	400	1500	–

[a]From Ref. [47].
[b]Sodium chloride solution of salinity $S = 0.1$, see Appendix C.
[c]From Sigma-Aldrich Production GmbH and Fluka data sheets.
[d]From Refs. [15,18].

As typical materials for the particles we have chosen to analyze the polymers polystyrene (PS), polymethacrylate (PM), and melamine resin (MR), as well as pyrex (PY) and a typical biological cell (Cell), see Table I.

B. Traveling acoustic waves

As mentioned above, our theory including viscosity predicts a strong enhancement of the acoustic radiation force by a factor of $(ka)^{-3}$ compared to the standard inviscid theory for the case of purely traveling waves. Here we analyze the case of a planar traveling wave with $\boldsymbol{k} = k\boldsymbol{e}_z$ and $p_1 = p_{\mathrm{a}}\mathrm{e}^{\mathrm{i}(kz-\omega t)}$. In this case the acoustic energy density E_{ac} of the wave is $E_{\mathrm{ac}} = \frac{1}{2}\kappa_0 p_{\mathrm{a}}^2$, and the radiation force (21) becomes

$$\boldsymbol{F}^{\mathrm{rad}} = \pi a^3 k f_2^{\mathrm{i}}(\tilde{\rho},\tilde{\delta})\,E_{\mathrm{ac}}\,\boldsymbol{e}_z. \tag{49}$$

For a 5-μm-diameter pyrex sphere in water at 1.5 MHz we have $a = 2.5\ \mu$m, $\tilde{\delta} = 0.23$, $k = 4.24\times 10^3$ m^{-1}, and $\tilde{\rho} = 2.23$. From Eq. (45) we find $f_2^{\mathrm{i}}(2.23,0.23) = 0.058$, and taking the typical acoustic energy density $E_{\mathrm{ac}} = 100$ J/m^3 [30], we arrive at $F^{\mathrm{rad}} \approx 1.2$ pN. Under the influence of this force, the pyrex sphere would reach the terminal translational velocity $v_{\mathrm{p}} = F^{\mathrm{rad}}/(6\pi\eta a) \approx 25\ \mu$m/s. This is a significant velocity for microchannel acoustophoresis, where typical velocities lie in the range from 5 to 500 μm/s [31]. In the standard inviscid theory [2,3], the estimate for the radiation force is a factor

of $(ka)^3 \approx 10^{-6}$ lower, corresponding to an acoustophoretic velocity smaller than 0.1 nm/s.

C. Standing acoustic waves

In many experiments on rectangular microfluidic channels with coplanar walls at $z = 0$ and $z = h$, the incoming wave have approximately been a resonant, standing one-dimensional (1D) pressure wave of the form $p_1 = p_a \cos(kz)$, with wave number $k = n\pi/h$, where n is the number of half wavelengths, and with the acoustic energy density $E_{ac} = \frac{1}{4}\kappa_0 p_a^2$. The expression for the radiation force then simplifies to the classic result by Yosioka and Kawasima [2],

$$F_{1D}^{rad} = 4\pi\ \Phi(\tilde{\kappa},\tilde{\rho},\tilde{\delta})\, a^3 k E_{ac} \sin(2kz), \tag{50a}$$

$$\Phi(\tilde{\kappa},\tilde{\rho},\tilde{\delta}) = \tfrac{1}{3}\ f_1(\tilde{\kappa}) + \tfrac{1}{2}\ f_2^r(\tilde{\rho},\tilde{\delta}), \tag{50b}$$

where the acoustophoretic contrast factor $\Phi(\tilde{\kappa},\tilde{\rho},\tilde{\delta})$ now depends on viscosity.

Experiments on suspended biological cells involve near-neutral-buoyant particles $|\tilde{\rho} - 1| \ll 1$, implying that the monopole coefficient $|f_1|$ is typically much larger than the dipole coefficient $|f_2^r|$. Because the acoustic contrast factor Φ defined in Eq. (50b) is a linear combination of the two scattering coefficients, a good quantitative measure of the ability to detect the effect of viscosity on the acoustic radiation force is therefore the relative change in Φ with and without viscosity. We therefore find it helpful to introduce the detectability measure $\mathcal{D}$ of viscous effects as

$$\mathcal{D}(\tilde{\kappa},\tilde{\rho},\tilde{\delta}) = \frac{\Phi(\tilde{\kappa},\tilde{\rho},\tilde{\delta}) - \Phi(\tilde{\kappa},\tilde{\rho},0)}{\Phi(\tilde{\kappa},\tilde{\rho},0)} \quad \text{or} \tag{51a}$$

$$1 + \mathcal{D}(\tilde{\kappa},\tilde{\rho},\tilde{\delta}) = \frac{\Phi(\tilde{\kappa},\tilde{\rho},\tilde{\delta})}{\Phi(\tilde{\kappa},\tilde{\rho},0)}. \tag{51b}$$

Examples of $\mathcal{D}$ for in NaCl solutions are shown in Fig. 3 going from nearly undetectable sub-1% levels for polystyrene spheres to above 10% levels for pyrex spheres.

The effect of including the viscosity in the expression for the acoustic radiation force can also be illustrated by contour plots of the contrast factor Φ in the $(\tilde{\rho},\tilde{\kappa})$ plane for fixed values of $\tilde{\delta}$ as shown in Fig. 4. The change in the contrast factor is clearly seen by the changing contour lines. While Φ is independent of $\tilde{\delta}$ along the neutral-buoyancy line $\tilde{\rho} = 1$, its value is increased when going from the inviscid case $\tilde{\delta} = 0$ in Fig. 4(a) to the viscous case $\tilde{\delta} = 1$ in Fig. 4(b). The change of the contour line $\Phi = 0.0$ is particularly interesting as particles on opposite side of this line move in opposite directions, and the plot of Φ in the $(\tilde{\rho},\tilde{\kappa})$ plane is therefore also useful when attempting to tune the solvent to obtain binary separation of particles. In Fig. 4, a number of specific examples of materials are marked by crosses. As particle material are chosen polystyrene (PS), polymethacrylate (PM), melamine resin (MR), and a typical biological cell (Cell), while the liquids are water (wa), glycerol (gl), and percoll (pc). Note that the Cell/gl and Cell/wa points lie on opposite sides of the zero contour. A curve connecting these two points would represent the acoustophoretic response of cells in various mixtures of glycerol and water. From a purely physical point of view, this system may therefore form an excellent tunable solvent with respect to obtaining binary separation of cells.

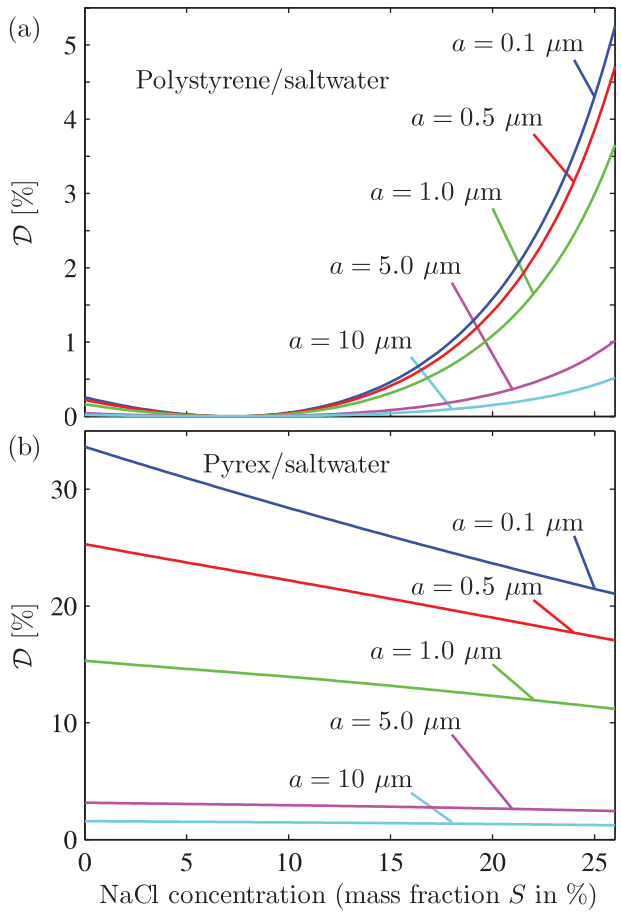

FIG. 3. (Color online) The detectability $\mathcal{D}$ for solid microspheres of radius a ranging from 0.1 to 10 μm in a sodium chloride solution as a function of NaCl concentration (mass fraction S), see Appendix A. (a) Polystyrene spheres for which $\mathcal{D}$ is typically a few percent or lower. (b) Pyrex spheres for which $\mathcal{D}$ easily can be larger than 10%.

The effect of viscosity can also be studied through vertical acoustic trapping [49,50], where the buoyancy force $F^{buoy} = (4\pi/3)(\tilde{\rho} - 1)\rho_0 a^3 g$ is balanced by a vertically oriented standing plane-wave acoustic field $\boldsymbol{F}^{rad} = F^{rad}\boldsymbol{e}_z$. For a given acoustic energy density E_{ac}, the maximal acoustic radiation force is given by the amplitude $4\pi\,\Phi(\tilde{\kappa},\tilde{\rho},\tilde{\delta})a^3 k E_{ac}$ in Eq. (50a). Based on this, the critical trapping force is defined as the threshold for obtaining vertical acoustic trapping using the smallest possible acoustic energy density E_{ac}^{min},

$$E_{ac}^{min} = \frac{|\tilde{\rho} - 1|}{3\Phi(\tilde{\kappa},\tilde{\rho},\tilde{\delta})}\,\frac{\rho_0 g}{k}. \tag{52}$$

The effect of viscosity can therefore be measured as

$$E_{ac}^{min}(\tilde{\delta}) = \frac{1}{1 + \mathcal{D}}\ E_{ac}^{min}(0). \tag{53}$$

A quantity more readily accessible experimentally may be the voltage U_{pz} used to drive the piezo transducer generating the ultrasound wave in a typical experiment. As E_{ac} scales with the square of U_{pz} [30], we have

$$U_{pz}(\tilde{\delta}) = \frac{1}{\sqrt{1 + \mathcal{D}}}\ U_{pz}(0). \tag{54}$$

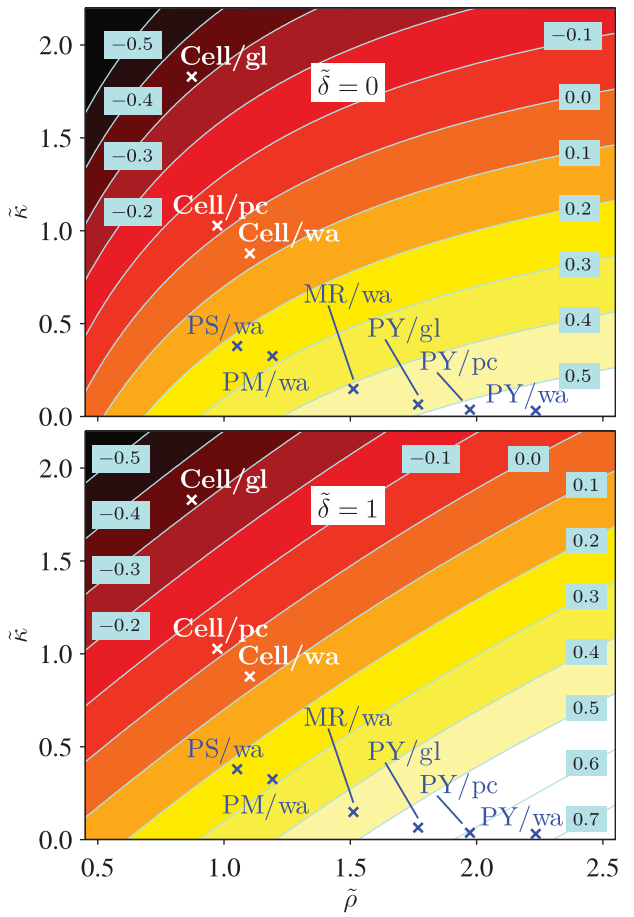

FIG. 4. (Color online) Contour plots of the acoustic contrast factor $\Phi(\tilde{\kappa},\tilde{\rho},\tilde{\delta})$ as function of $\tilde{\kappa}$ and $\tilde{\rho}$ for fixed values of $\tilde{\delta}$, from $\Phi < -0.5$ (black) to $\Phi > 0.5$ (white) in steps of 0.1. The position in the $(\tilde{\rho},\tilde{\kappa})$ plane for various material parameters are marked by crosses and the following labels: polystyrene (PS), polymethacrylate (PM), melamine resin (MR), a typical biological cell (Cell), water (wa), glycerol (gl), and percoll (pc). (a) The inviscid case $\tilde{\delta} = 0$. (b) The viscous case $\tilde{\delta} = 1$.

Here the detectability $\mathcal{D}$ of Fig. 3 appears directly. The complex frequency and temperature dependence of the piezo transducer response to $U_{\rm pz}$ complicates the matter [32,51]. However, the use of low voltages, transducers with medium-range Q values, and active temperature control [31] would make this a viable method.

VI. CONCLUSION

We have derived an analytical expression for the acoustic radiation force in the long-wavelength limit $\delta, a \ll \lambda$ on a compressible, spherical particle of radius a suspended in a liquid with viscous penetration depth δ.

We have analyzed the experimental predictions provided by our expression for traveling waves and for standing waves. In the case of the former we find a strong enhancement proportional to $(ka)^{-3} \approx 10^6$ relative to the inviscid case due to nonvanishing interference between the incoming wave and the scattered wave. For standing waves we have found a negligible sub-1% deviation from the inviscid result for large (micrometer-sized), nearly neutral-buoyancy particles, such as biological cells in water. However, significant deviations above 10% from the inviscid result were found for buoyant particles, such as pyrex in water. The smaller the particle radius a is relative to the viscous boundary-layer thickness δ, the larger the effect of viscosity.

It should be possible using state-of-the-art instrumentation for microchannel acoustophoresis, such as the automated micro-PIV setup recently published by Augustsson *et al.* [31], to experimentally test the predictions presented in this paper.

ACKNOWLEDGMENTS

We thank Per Augustsson, Lund University, and Rune Barnkob, Technical University of Denmark, for assisting us in collecting the parameter values listed in Table I. This work was supported in part by the Danish Council for Independent Research, Technology and Production Sciences, Grant No. 274-09-0342.

APPENDIX A: MATHEMATICAL DETAILS IN DERIVING THE DEPENDENCE OF $F^{\rm rad}$ ON $\nabla p_{\rm in}$ AND $v_{\rm in}$

To derive Eq. (18) we use the index notation (including summation of repeated indices). Keeping only the mixed terms proportional to $\phi_{\rm in}\phi_{\rm sc}$ representing interference between the incoming and the scattered wave, the ith component of Eq. (14) becomes

$$F_i^{\rm rad} = -\int_{\partial\Omega} da\, n_j \left\{ \left[\frac{c_0^2}{\rho_0} \langle \rho_{\rm in}\rho_{\rm sc}\rangle - \rho_0 \langle v_k^{\rm in} v_k^{\rm sc}\rangle \right]\delta_{ij} + \rho_0 \langle v_i^{\rm in} v_j^{\rm sc}\rangle + \rho_0 \langle v_i^{\rm sc} v_j^{\rm in}\rangle \right\} \tag{A1a}$$

$$= -\int_{\Omega} d\boldsymbol{r}\, \partial_j \left\{ \left[\frac{c_0^2}{\rho_0} \langle \rho_{\rm in}\rho_{\rm sc}\rangle - \rho_0 \langle v_k^{\rm in} v_k^{\rm sc}\rangle \right]\delta_{ij} + \rho_0 \langle v_i^{\rm in} v_j^{\rm sc}\rangle + \rho_0 \langle v_i^{\rm sc} v_j^{\rm in}\rangle \right\} \tag{A1b}$$

$$= -\int_{\Omega} d\boldsymbol{r} \left\{ \frac{c_0^2}{\rho_0} \left[\langle \rho_{\rm in}\partial_i \rho_{\rm sc}\rangle + \langle \rho_{\rm sc}\partial_i \rho_{\rm in}\rangle \right] + \rho_0 \left[\langle v_i^{\rm in}\partial_j v_j^{\rm sc}\rangle + \langle v_i^{\rm sc}\partial_j v_j^{\rm in}\rangle \right] \right\} \tag{A1c}$$

$$= -\int_{\Omega} d\boldsymbol{r} \left\{ -\langle \rho_{\rm in}\partial_t v_i^{\rm sc}\rangle - \langle \rho_{\rm sc}\partial_t v_i^{\rm in}\rangle + \rho_0 \langle v_i^{\rm in}\partial_j v_j^{\rm sc}\rangle - \langle v_i^{\rm sc}\partial_t \rho_{\rm in}\rangle \right\} \tag{A1d}$$

$$= -\int_{\Omega} d\boldsymbol{r} \left\{ \langle v_i^{\rm in}\partial_t \rho_{\rm sc}\rangle + \rho_0 \langle v_i^{\rm in}\partial_j v_j^{\rm sc}\rangle \right\} \tag{A1e}$$

$$= -\int_{\Omega} d\boldsymbol{r}\, \rho_0 \left\langle v_i^{\rm in} \left(\partial_j^2 \phi_{\rm sc} - \frac{1}{c_0^2}\partial_t^2 \phi_{\rm sc} \right) \right\rangle, \tag{A1f}$$

which is Eq. (18). Here, showing details not explained in Ref. [3], we have used $p_1 = c_0^2 \rho_1$ in Eq. (A1a), Gauss's theorem in Eq. (A1b), exchange of indices $\partial_i v_k = \partial_i \partial_k \phi = \partial_k \partial_i \phi = \partial_k v_i$ to cancel terms in Eq. (A1c), introduction of time derivatives by the continuity equation $\partial_t \rho_1 = -\rho_0 \partial_j v_{1,j}$ and the Navier–Stokes equation $\rho_0 \partial_t v_{1,i} = -\partial_i p_1 = -c_0^2 \partial_i \rho_1$ in Eq. (A1d), vanishing of time-averages of total time derivatives $\langle \partial_t(\rho v_i)\rangle = 0$ or $\langle \rho \partial_t v_i\rangle = -\langle v_i \partial_t \rho\rangle$ for cancellation and

rearrangement in Eq. (A1e), and finally reintroduction of the vector potential ϕ_{sc} in Eq. (A1f).

To derive Eq. (19) we note that the d'Alembert wave operator $\partial_j^2 - (1/c_0^2)\partial_t^2$ appears in the integrand of Eq. (A1f) and acts on ϕ_{sc}, and because ϕ_{sc} is a sum of simple monopole and dipole terms, significant simplifications are possible. Just as the Laplace operator acting on the monopole potential $\phi = q/(4\pi\epsilon_0 r)$ yields the point-charge distribution $\partial_j^2\phi = -(q/\epsilon_0)\delta(\boldsymbol{r})$ in the static case, the d'Alembert operator acting on the retarded-time monopole and dipole expressions (17) also yields δ function distributions,

$$\left[\partial_j^2 - \frac{1}{c_0^2}\partial_t^2\right]\phi_{sc} = f_1\,\frac{4\pi a^3}{3\rho_0}\,\partial_t\rho_{in}\,\delta(\boldsymbol{r}) + f_2\,2\pi a^3\,\boldsymbol{\nabla}\cdot[\boldsymbol{v}_{in}\,\delta(\boldsymbol{r})], \quad r \gg \lambda. \tag{A2}$$

Now we see the great advantage of working in the far-field limit. The first term is easily integrated, when appearing in Eq. (A1f), but for the second term we need to get rid of the divergence operator acting on the δ function before we can evaluate the integral. This we manage by Gauss' theorem. First we note that $\boldsymbol{\nabla}\cdot[v(\boldsymbol{r})\boldsymbol{u}(\boldsymbol{r})] = v\boldsymbol{\nabla}\cdot\boldsymbol{u} + \boldsymbol{u}\cdot\boldsymbol{\nabla}v$ for any scalar function v and vector function $\boldsymbol{u}$. Therefore, $\int_{\partial\Omega} da\,\boldsymbol{n}\cdot(v\boldsymbol{u}) = \int_\Omega d\boldsymbol{r}\,\boldsymbol{\nabla}\cdot(v\boldsymbol{u}) = \int_\Omega d\boldsymbol{r}\,(v\boldsymbol{\nabla}\cdot\boldsymbol{u} + \boldsymbol{u}\cdot\boldsymbol{\nabla}v)$, and we have derived the expression $\int_\Omega d\boldsymbol{r}\,v\boldsymbol{\nabla}\cdot\boldsymbol{u} = -\int_\Omega d\boldsymbol{r}\,\boldsymbol{u}\cdot\boldsymbol{\nabla}v + \int_{\partial\Omega} da\,\boldsymbol{n}\cdot(v\boldsymbol{u})$. Now, since $\boldsymbol{u} \propto \boldsymbol{v}\delta(\boldsymbol{r})$ we obtain in Eq. (A1f) a volume integral encompassing the δ function, thus yielding a nonzero contribution, and a surface integral avoiding the δ function, thus yielding zero. Consequently, the resulting expression for $\boldsymbol{F}^{rad}$ becomes

$$\boldsymbol{F}^{rad} = -\frac{4\pi}{3}a^3\,\langle f_1\boldsymbol{v}_{in}\partial_t\rho_{in}\rangle + 2\pi a^3\rho_0\,\langle f_2(\boldsymbol{v}_{in}\cdot\boldsymbol{\nabla})\boldsymbol{v}_{in}\rangle \tag{A3a}$$

$$= \frac{4\pi}{3}a^3\,\langle f_1\rho_{in}\partial_t\boldsymbol{v}_{in}\rangle + 2\pi a^3\rho_0\,\langle f_2(\boldsymbol{v}_{in}\cdot\boldsymbol{\nabla})\boldsymbol{v}_{in}\rangle \tag{A3b}$$

$$= -\frac{4\pi}{3\rho_0 c_0^2}a^3\,\langle f_1 p_{in}\boldsymbol{\nabla}p_{in}\rangle + 2\pi a^3\,\rho_0\langle f_2\boldsymbol{v}_{in}\cdot\boldsymbol{\nabla}\boldsymbol{v}_{in}\rangle \tag{A3c}$$

$$= -\pi a^3\left[\frac{2\kappa_0}{3}\mathrm{Re}[f_1^* p_{in}^*\boldsymbol{\nabla}p_{in}] - \rho_0\mathrm{Re}[f_2^*\boldsymbol{v}_{in}^*\cdot\boldsymbol{\nabla}\boldsymbol{v}_{in}]\right], \quad \text{with } p_{in} \text{ and } \boldsymbol{v}_{in} \text{ evaluated at } \boldsymbol{r} = \boldsymbol{0}, \tag{A3d}$$

which is Eq. (19). Here we have integrated over the δ function in Eq. (A3a), applied the previously used rule $\langle\rho_{in}\partial_t\boldsymbol{v}_{in}\rangle = -\langle\boldsymbol{v}_{in}\partial_t\rho_{in}\rangle$ in Eq. (A3b), inserted $\rho_{in} = p_{in}/c_0^2$ and $\partial_t\boldsymbol{v}_{in} = -\boldsymbol{\nabla}p_{in}/\rho_0$ in Eq. (A3c), and finally taken the time average using Eq. (11) in Eq. (A3d).

APPENDIX B: MATHEMATICAL DETAILS CONCERNING THE STREAM FUNCTION $\Psi(r,\theta)$

The incompressibility of the velocity field $\boldsymbol{v}_{ab}$ [Eq. (31)] is ensured, because $\boldsymbol{\nabla}\cdot\boldsymbol{v}_{ab} = \boldsymbol{\nabla}\cdot(\boldsymbol{\nabla}\times[\Psi\boldsymbol{e}_\phi]) = 0$ for any Ψ. To show that $\Psi = \Psi_1 + \Psi_2$ is a solution if Ψ_1 and Ψ_2 obey Eqs. (32) and (33), respectively, we insert $\boldsymbol{v}_{ab}$ of Eq. (31) into the first-order Navier-Stokes equation (6b) and take the rotation. This results in $-i\omega\rho_0\boldsymbol{\nabla}\times\boldsymbol{v}_{ab} = \eta\nabla^2(\boldsymbol{\nabla}\times\boldsymbol{v}_{ab})$, and because Ψ is independent of ϕ, we have $\boldsymbol{\nabla}\times\boldsymbol{v}_{ab} = \boldsymbol{\nabla}\times[\boldsymbol{\nabla}\times(\Psi\boldsymbol{e}_\phi)] = -\nabla^2(\Psi\boldsymbol{e}_\phi)$ and arrive at

$$\nabla^2(\nabla^2 + q^2)[\Psi(r,\theta)\,\boldsymbol{e}_\phi] = \boldsymbol{0}, \quad \text{with} \quad q = \frac{1+i}{\delta}. \tag{B1}$$

Introducing $\Psi(r,\theta) = \Psi_1(r,\theta) + \Psi_2(r,\theta)$, we obtain

$$\nabla^2(\nabla^2 + q^2)[(\Psi_1 + \Psi_2)\,\boldsymbol{e}_\phi] = \boldsymbol{0}, \tag{B2a}$$

if Ψ_1 and Ψ_2 satisfy the following conditions:

$$\nabla^2(\Psi_1\boldsymbol{e}_\phi) = \boldsymbol{0}, \tag{B2b}$$

$$(\nabla^2 + q^2)(\Psi_2\boldsymbol{e}_\phi) = \boldsymbol{0}. \tag{B2c}$$

For any ϕ-independent function $\Psi(r,\theta)$ we obtain $\nabla^2[\Psi(r,\theta)\,\boldsymbol{e}_\phi] = [\nabla^2\Psi - \Psi/(r\sin\theta)^2]\,\boldsymbol{e}_\phi$, and Eqs. (B2b) and (B2c) reduce to Eqs. (32) and (33), respectively.

Finally, once $\Psi(r,\theta)$ is written in the form Eq. (37), the velocity components Eq. (36) are obtained from using

$$\boldsymbol{v}_{ab} = \boldsymbol{\nabla}\times[\Psi\,\boldsymbol{e}_\phi] = \frac{\partial_\theta(\sin\theta\,\Psi)}{r\sin\theta}\,\boldsymbol{e}_r - \frac{\partial_r(r\,\Psi)}{r}\,\boldsymbol{e}_\theta. \tag{B3}$$

APPENDIX C: MATERIAL PARAMETERS OF NACL SOLUTIONS

In the following we summarize parameter values for the speed of sound c_{scs}, the density ρ_{scs}, and the viscosity η_{scs} of sodium chloride solutions (NaCl in water) as a function of temperature T (in °C) and mass fraction S of NaCl in the solution (salinity). The salinity ranges from zero in pure water to a maximum of 0.26 in a saturated solution.

The speed of sound $c_{scs}(S,T)$ in NaCl/water solutions is given by Kleis and Sanchez [52] as

$$c_{scs}(S,T) = \sum_{j=0}^{4}(a_j + b_j S)\left[\frac{T}{1°C}\right]^j \mathrm{m\,s^{-1}}, \tag{C1}$$

where the coefficients a_j and b_j are

$$\begin{aligned} a_0 &= 1.403\,09\times10^3, & b_0 &= 1.401\,90\times10^3,\\ a_1 &= 4.683\,91\times10^0, & b_1 &= -1.149\,96\times10^1,\\ a_2 &= -4.053\,88\times10^{-2}, & b_2 &= 2.237\,48\times10^{-3},\\ a_3 &= 1.295\,50\times10^{-5}, & b_3 &= 1.482\,38\times10^{-3},\\ a_4 &= 6.914\,85\times10^{-7}, & b_4 &= -9.461\,65\times10^{-6}. \end{aligned} \tag{C2}$$

The density $\rho_{scs}(S,T)$ of sodium chloride solutions is given by Laliberté and Cooper [53] as

$$\rho_{scs}(S,T) = \frac{\rho_{wa}(T)}{1 - S + S\,V_{app}(S,T)\rho_{wa}(T)}, \tag{C3}$$

where the density $\rho_{wa}(T)$ of water is given by

$$\rho_{wa}(T) = \frac{1}{1 + d\frac{T}{1°C}}\sum_{j=0}^{5} d_j\left[\frac{T}{1°C}\right]^j \mathrm{kg\,m^{-3}}, \tag{C4}$$

with the coefficients d and d_j being

$$\begin{aligned} d &= 1.687\,985\,0 \times 10^{-2}, \\ d_0 &= 9.998\,395\,2 \times 10^{2}, \quad & d_3 &= -4.617\,046\,1 \times 10^{-5}, \\ d_1 &= 1.694\,517\,6 \times 10^{1}, \quad & d_4 &= 1.055\,630\,2 \times 10^{-7}, \\ d_2 &= -7.987\,040\,1 \times 10^{-3}, \quad & d_5 &= -2.805\,425\,3 \times 10^{-10}, \end{aligned} \tag{C5}$$

and where the apparent specific volume $V_{\text{app}}(S,T)$ of NaCl is given by

$$V_{\text{app}}(S,T) = \frac{S + e_2 + e_3 \frac{T}{1^\circ\text{C}}}{(e_0 S + e_1)\,\exp\left[e_5\left(\frac{T}{1^\circ\text{C}} + e_4\right)^2\right]}\ \text{m}^3\ \text{kg}^{-1}, \tag{C6}$$

with the coefficients e_j being

$$\begin{aligned} e_0 &= -4.330 \times 10^{-2}, \quad & e_3 &= 1.4624 \times 10^{-2}, \\ e_1 &= 6.471 \times 10^{-2}, \quad & e_4 &= 3.3156 \times 10^{3}, \\ e_2 &= 1.016\,60 \times 10^{0}, \quad & e_5 &= 1.0000 \times 10^{-6}. \end{aligned} \tag{C7}$$

The viscosity $\eta_{\text{scs}}(S,T)$ of NaCl/water solutions is given by Laliberté [54] as

$$\eta_{\text{scs}}(S,T) = [\eta_{\text{wa}}(T)]^{(1-S)}\,[\eta_{\text{NaCl}}(S,T)]^{S}, \tag{C8}$$

where the viscosities $\eta_{\text{wa}}(T)$ and $\eta_{\text{NaCl}}(S,T)$ of water and liquid NaCl, respectively, are

$$\eta_{\text{wa}}(T) = \frac{\left[\frac{T}{1^\circ\text{C}} + 246\right]\ \text{mPa s}}{\left[0.05594\frac{T}{1^\circ\text{C}} + 5.2842\right]\frac{T}{1^\circ\text{C}} + 137.37}, \tag{C9}$$

$$\eta_{\text{NaCl}}(S,T) = \exp\left[\frac{h_1 S^{h_2} + h_3}{\left[1 + h_4\frac{T}{1^\circ\text{C}}\right]\,[1 + h_5 S^{h_6}]}\right]\text{mPa s}, \tag{C10}$$

with the coefficients h_j being

$$\begin{aligned} h_1 &= 1.6220 \times 10^{1}, \quad & h_4 &= 7.4691 \times 10^{-3}, \\ h_2 &= 1.3229 \times 10^{0}, \quad & h_5 &= 3.0780 \times 10^{1}, \\ h_3 &= 1.4849 \times 10^{0}, \quad & h_6 &= 2.0583 \times 10^{0}. \end{aligned} \tag{C11}$$

[1] L. V. King, Phys. R. Soc. London A Mat **147**, 212 (1934).
[2] K. Yosioka and Y. Kawasima, Acustica **5**, 167 (1955).
[3] L. P. Gorkov, Sov. Phys. Dokl. **6**, 773 (1962).
[4] F. Petersson, A. Nilsson, C. Holm, H. Jönsson, and T. Laurell, Analyst **129**, 938 (2004).
[5] F. Petersson, A. Nilsson, C. Holm, H. Jönsson, and T. Laurell, Lab Chip **5**, 20 (2005).
[6] J. J. Hawkes, R. W. Barber, D. R. Emerson, and W. T. Coakley, Lab Chip **4**, 446 (2004).
[7] J. Hultström, O. Manneberg, K. Dopf, H. M. Hertz, H. Brismar, and M. Wiklund, Ultrasound Med. Biol. **33**, 145 (2007).
[8] M. Evander, L. Johansson, T. Lilliehorn, J. Piskur, M. Lindvall, S. Johansson, M. Almqvist, T. Laurell, and J. Nilsson, Anal Chem **79**, 2984 (2007).
[9] J. Svennebring, O. Manneberg, P. Skafte-Pedersen, H. Bruus, and M. Wiklund, Biotechnol. Bioeng. **103**, 323 (2009).
[10] A. Lenshof, A. Ahmad-Tajudin, K. Jaras, A.-M. Sward-Nilsson, L. Aberg, G. Marko-Varga, J. Malm, H. Lilja, and T. Laurell, Anal Chem **81**, 6030 (2009).
[11] J. V. Norris, M. Evander, K. M. Horsman-Hall, J. Nilsson, T. Laurell, and J. P. Landers, Anal Chem **81**, 6089 (2009).
[12] C. Grenvall, P. Augustsson, J. R. Folkenberg, and T. Laurell, Anal Chem **81**, 6195 (2009).
[13] T. Franke, S. Braunmueller, L. Schmid, A. Wixforth, and D. A. Weitz, Lab Chip **10**, 789 (2010).
[14] P. Thevoz, J. D. Adams, H. Shea, H. Bruus, and H. T. Soh, Anal Chem **82**, 3094 (2010).
[15] P. Augustsson, R. Barnkob, C. Grenvall, T. Deierborg, P. Brundin, H. Bruus, and T. Laurell, in *Proc. 14th MicroTAS, 3–7 October 2010, Groningen, The Netherlands*, edited by S. Verporte, H. Andersson, J. Emneus, and N. Pamme (CBMS, 2010), pp. 1337–1339.
[16] D. Hartono, Y. Liu, P. L. Tan, X. Y. S. Then, L.-Y. L. Yung, and K.-M. Lim, Lab Chip **11**, 4072 (2011).
[17] S. M. Hagsäter, T. G. Jensen, H. Bruus, and J. P. Kutter, Lab Chip **7**, 1336 (2007).
[18] J. Shi, X. Mao, D. Ahmed, A. Colletti, and T. J. Huang, Lab Chip **8**, 221 (2008).
[19] J. Shi, H. Huang, Z. Stratton, Y. Huang, and T. J. Huang, Lab Chip **9**, 3354 (2009).
[20] M. K. Tan, R. Tjeung, H. Ervin, L. Y. Yeo, and J. Friend, Appl. Phys. Lett. **95**, 134101 (2009).
[21] M. K. Tan, L. Y. Yeo, and J. R. Friend, Appl. Phys. Lett. **97**, 234106 (2010).
[22] J. Shi, S. Yazdi, S.-C. S. Lin, X. Ding, I.-K. Chiang, K. Sharp, and T. J. Huang, Lab Chip **11**, 2319 (2011).
[23] O. Manneberg, S. M. Hagsäter, J. Svennebring, H. M. Hertz, J. P. Kutter, H. Bruus, and M. Wiklund, Ultrasonics **49**, 112 (2009).
[24] O. Manneberg, B. Vanherberghen, B. Onfelt, and M. Wiklund, Lab Chip **9**, 833 (2009).
[25] P. Glynne-Jones, R. J. Boltryk, N. R. Harris, A. W. J. Cranny, and M. Hill, Ultrasoncis **50**, 68 (2010).
[26] J. D. Adams, P. Thevoz, H. Bruus, and H. T. Soh, Appl. Phys. Lett. **95**, 254103 (2009).
[27] S. Oberti, D. Moeller, A. Neild, J. Dual, F. Beyeler, B. J. Nelson, and S. Gutmann, Ultrasonics **50**, 247 (2010).
[28] C. Ratier and M. Hoyos, Anal Chem **82**, 1318 (2010).
[29] J. D. Adams and H. T. Soh, Appl. Phys. Lett. **97**, 064103 (2010).
[30] R. Barnkob, P. Augustsson, T. Laurell, and H. Bruus, Lab Chip **10**, 563 (2010).
[31] P. Augustsson, R. Barnkob, S. T. Wereley, H. Bruus, and T. Laurell, Lab Chip **11**, 4152 (2011).
[32] J. Friend and L. Y. Yeo, Rev. Mod. Phys. **83**, 647 (2011).
[33] H. Bruus, J. Dual, J. Hawkes, M. Hill, T. Laurell, J. Nilsson, S. Radel, S. Sadhal, and M. Wiklund, Lab Chip **11**, 3579 (2011).
[34] L. Rayleigh, Philos. Trans. R. Soc. London **175**, 1 (1884).
[35] L. D. Landau and E. M. Lifshitz, *Fluid Mechanics*, 2nd ed., Vol. 6, Course of Theoretical Physics (Pergamon, Oxford, 1993).

[36] A. Doinikov, J. Acoust. Soc. Am. **101**, 722 (1997).
[37] S. Danilov and M. Mironov, J. Acoust. Soc. Am. **107**, 143 (2000).
[38] J. Lighthill, *Waves in Fluids* (Cambridge University Press, Cambridge, 2002).
[39] A. D. Pierce, *Acoustics* (Acoustical Society of America, Woodbury, NY, 1991).
[40] H. Bruus, Lab Chip **11**, 3742 (2011).
[41] P. M. Morse and K. U. Ingard, *Theoretical Acoustics* (Princeton University Press, Princeton NJ, 1986).
[42] J. D. Jackson, *Classical Electrodynamics*, 2nd ed. (Wiley and Sons, New York, 1975).
[43] M. D. Van Dyke, *Perturbation Methods in Fluid Mechanics*, 2nd ed. (Parabolic, Stanford CA, 1975).
[44] M. Weiser and R. Apfel, J. Acoust. Soc. Am. **71**, 1261 (1982).
[45] R. J. Urick, J. Acoust. Soc. Am. **20**, 283 (1948).
[46] T. Laurent, H. Pertoft, and O. Nordli, J. Colloid Interface Sci. **76**, 124 (1980).
[47] C. Product, *CRC Handbook of Chemistry and Physics*, 90th ed. (Taylor and Francis, New York, 2010).
[48] M. Godin, A. K. Bryan, T. P. Burg, K. Babcock, and S. R. Manalis, Appl. Phys. Lett. **91**, 123121 (2007).
[49] R. Apfel, J. Acoust. Soc. Am. **59**, 339 (1976).
[50] M. Kumar, D. Feke, and J. Belovich, Biotechnol. Bioeng. **89**, 129 (2005).
[51] J. Dual and D. Möller, Lab Chip **12**, 506 (2012).
[52] S. Kleis and L. Sanchez, Solar Energy **45**, 201 (1990).
[53] M. Laliberté and W. Cooper, J. Chem. Eng. Data **49**, 1141 (2004).
[54] M. Laliberté, J. Chem. Eng. Data **52**, 1507 (2007).